N89-29871

4.3 MEASUREMENTS OF TURBULENCE AND ITS EVOLUTION AND VARIABILITY DURING MAP

W. K. Hocking

Department of Physics and Mathematical Physics
University of Adelaide, GPO Box 498
Adelaide, S. A. 5001, Australia

The understanding of turbulence in the middle atmosphere has improved considerably during the MAP period. For a theoretical viewpoint, several advances have been made including understanding the ways in which turbulence is generated, and the differences between the rates of diffusion of momentum and heat. Experimentally, a proper understanding of how radars can be used to measure turbulence has emerged, and turbulent energy dissipation rates in the middle atmosphere have been measured with MF, HF, and VHF radars. New rocket techniques have been developed which have enabled detailed studies of the fine structure of turbulence to be made. Whilst some discrepancies between techniques still exist, these will undoubtedly be resolved soon, and these different techniques are already providing a great improvement in the understanding of turbulence on a global scale. It is to be hoped that the years following MAP will be as productive as the years of MAP, and that these improvements can be built on to provide even greater understanding.

1. Visualization of Turbulence

Although turbulence is in general associated with some sort of chaotic behavior, its visualization differs from scientist to scientist. To some, the details of the fine scale structure are completely unimportant, and turbulence is represented by a simple "K" term in the fluid dynamical equations, viz.

$$K \frac{\partial^2 u}{\partial z^2} \tag{1}$$

and similar terms (Figure 1). These "K" coefficients hide a multitude of sins, and represent perhaps the coursest visualization of turbulence. No heed is paid to the time scales involved in mixing processes, and K represents simply a coefficient which determines how "well" the fluid mixes. Nevertheless, for many workers this simple visualization seems adequate. An only slightly more sophisticated approach involves comparing the mixing of a turbulent field with the mixing which occurs at a molecular level in a gas, and a "diffusion coefficient" D is defined through the relations like

$$\sigma_z^2 = 2 D t \tag{2}$$

Here, σ_z^2 represents the mean square vertical displacement of an originally compact array of parcels which spreads out over time t. The analogy with molecular processes is quite poor, however, and if indeed σ_z^2 does vary proportionally to t it is more fortuitous than rigorous. Nevertheless, this representation does at least attempt to consider the time scales associated with the turbulent mixing, something that (1) does not.

More refined consideration of the temporal variation of σ_z^2 with respect to time shows that (2) is incorrect, because as the particles diffuse apart, larger scale motions become effective, hastening the process. In fact

$$\sigma_z^2 \approx \beta \varepsilon t^3 \tag{3}$$

more accurately describes the diffusive process, although the power of t depends largely on the spectrum of scales within the turbulent area.

Approaches to Turbulence

1. K-theory

$$K\frac{\partial^2 u}{\partial z^2} \quad \text{etc.}$$

$$(\rho\overline{u'w'} = -\rho K_m \frac{\partial u}{\partial z})$$

2. Molecular "analogy"

$$\sigma_z^2 = 2Dt$$

3. More refined

$$\sigma_z^2 \approx \beta\varepsilon t^3$$

4. Examination of fine detail
   - intermittency
   - structure of "eddies", etc.

5. New perspectives on turbulence and turbulent diffusion
   - Stokes diffusion
   - Deterministic chaos

Figure 1. Measurements of turbulence and its evolution and variability during MAP.

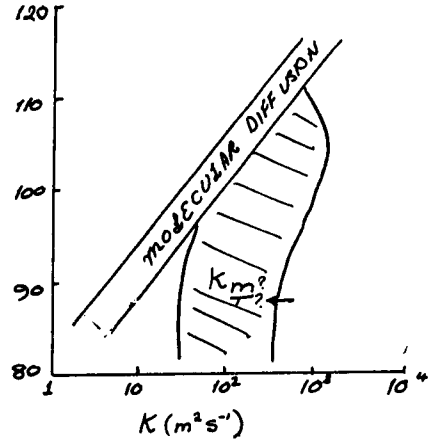

Figure 2. From Hocking [1987].

2. The "Gross" Approach

These types of "gross overview" descriptions, in which only the consequences of turbulence are important, and its detail is not, shall be referred to as "gross" views.

Many attempts have been made to make estimates of "K" in the middle atmosphere, largely by utilizing equations like (1). For example, one can generate equations which describe momentum and fluid motions in the atmosphere, leaving "K" as an "unknown" variable, and then proceed to use measurements of other known quantities like wind speeds, temperature distribution, and gravity wave fluxes to infer values for K. One of the most recent and best-known attempts at this is the model due to Garcia and Solomon [1985].

It is also possible to include chemistry in these models, and use measurements of concentration of atomic and molecular species to infer values for K. Early attempts at this include papers by Johnson and Wilkins [1965], Colegrove et al. [1965] and others. These authors looked in particular at the relative concentration of atomic oxygen and molecular oxygen at 90 and 120 km to infer information about K. More recently Groves [1986] has done similar things. When this type of approach is adopted, profiles of K as a function of height can be deduced. Figure 2 shows the range of values within which most measurements lie.

When one begins to consider these "diffusion" coefficients a little more carefully, however, it becomes clear that it is necessary to distinguish different types of K values. The diffusion coefficient for momentum is different from that for temperature, for example, and one needs to define K_T and K_m as separate entities. The rates between them, $P_r = K_m/K_t$, is called thePrandtl number. The estimates made by Garcia and Solomon, for example, represent estimates of K_m. The measurements in Figure 2 represent K_T. Values of K_m estimated by Garcia and Solomon agree with the profile for K_T in Figure 2. However, recently Strobel et al. [1987] have carefully constructed a computer model involving as much atmospheric chemistry as possible. They assumed a variety of forms for K_T and compared resultant profiles of minor species to measured values. An example is shown in Figure 3, for four different model K_T profiles. As a conclusion of their results, Figure 4 shows the acceptable range of K_T values which they deduced. The values are clearly less, by an order of magnitude, than those indicated earlier, and also less than the values for K_m inferred by Garcia and Solomon. Strobel et al. have taken this to infer that the Prandtl number in the middle atmosphere is about 10, a significant result. But before one accepts this argument, several issues need to be answered.

First, early estimates of the K_T by Johnson and Wilkins [1965] give much larger values for K_T, as do more recent estimates by Groves [1988]. It is certainly easy to dismiss the early results as being incorrect, due to the lack of sophistication of their models. However, Strobel's results show K_T to be much less than the molecular diffusion coefficient ν, so $(K_T + \nu)$ is $\sim \nu$. The results are very insensitive above 85 km, so we can only make use of these data below that height.

3. A Closer Look

Often this gross view is inadequate however. Even for workers who only need to know an estimate of K, it is useful to look closer at the turbulence causing the diffusion. To some, turbulence is visualized as a homogeneous process acting everywhere, something like the process in the atmospheric boundary layer, and that diffusion occurs simply because of this. Inertial range turbulence theory is adequate for such a model. In such a turbulent patch, it is possible to show that an individual cloud of particles which are initially close together diffuse apart in a manner

$$\sigma^2 = \beta \varepsilon t^3 \qquad (4)$$

as already discussed. One can then develop models around such a visualization.

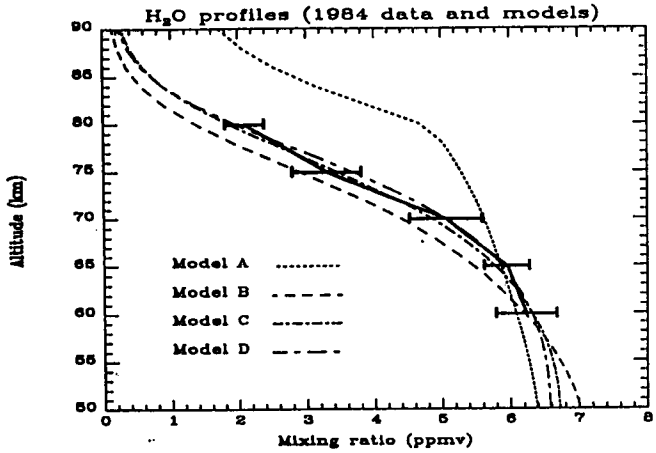

Figure 3. From Strobel et al., [1987].

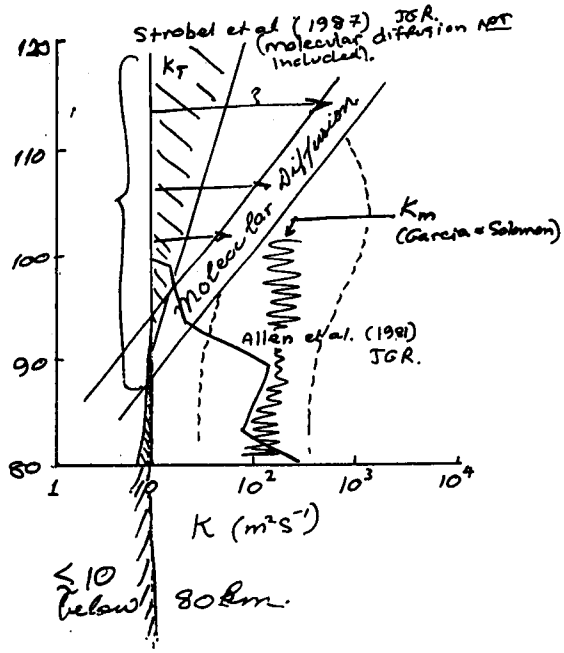

Figure 4.

Unfortunately, however, the middle atmosphere is not so simple! (In fact, turbulence generally is not.) Rather than being a homogeneous process acting uniformly throughout the region, it has been clearly shown through the MAP period that turbulence is both temporally and spatially intermittent. It occurs only for short periods of time at varying spatial locations. This is shown particularly well by Figures 5, 6, and 7 which show the occurrence of turbulent events in the upper troposphere and lower stratosphere. Clearly, events occur intermittently and last for varying lengths of time. Turbulent layers also have varying depths and spatial extents.

It appears that most of the turbulence is due to gravity waves and tides, and especially due to the superposition of gravity waves. The waves add up in such a way that R_i drops below 0.25, and even 0.0, producing instability. Fritts and Rastogi [1985] have shown that convective breakdown seems to be the major cause especially at high ω. Desaubies and Smith [1982] have modeled the results of an ensemble of gravity waves adding together, and do indeed find that a random distribution of breaking heights, times, and layer depths result. Figures 8 and 9 are for oceans, but similar concepts apply in the atmosphere.

The consequences of this intermittency are important. They mean, for example, that we must revisualize how large-scale turbulent diffusion takes place. An important proposal due to Dewan [1981], VanZandt and later Woodman and Rastogi [1984] suggested that the random occurrence of layers acts like a Monte Carlo process gradually causing diffusion, as first one layer forms, causing diffusion, and later another forms to cause transport over the depth of that layer. Thus the factors which control the large-scale diffusion are not the rates of diffusion across individual layers, but the frequency of occurrence and depth of individual layers (Figure 10).

Other consequences of the intermittency of turbulence include the possibility that the average rates of diffusivity of momentum and heat may be different, and that the Prandtl number may exceed 1, and perhaps be in the range 1 to 3 [Fritts and Dunkerton, 1985]. This is to say that if one parameterizes the rate of heat transport as $\alpha K_t (\partial\theta/\partial z)$, where $\partial\theta/\partial z$ is the mean temperature gradient, ignoring the effects of the wave on the mean, then the effective diffusive coefficient which must be used to describe the rate of diffusion is less than it would be if we properly included the effect of the wave in $\partial\theta/\partial z$. This is not so for momentum diffusion, because $\overline{u'w'}$ are not in phase quadrature.

4. Measurements of Turbulence

At this level of understanding, we have sufficient knowledge to make useful measurements of turbulence intensities. The three most direct techniques for measurements of turbulent energy dissipation rates used during the MAP period were based on balloons (stratosphere), rockets and radar experiments. There are many many subtleties associated with these techniques which I do not wish to dwell on here. They include such aspects as radar beam-broadening, layer thickness, and ion-neutral density mixing ratios. Other effects are also important as balloons can only be launched in quiet conditions, etc. Nevertheless, useful measurements have been made. For example, Barat [1982] and colleagues measured detailed temperature and velocity fluctuation in the stratosphere with balloon-borne anenometers (Figure 11). They found that the resultant structure function showed at least some ranges which an $r^{2/3}$ law held (Figure 12) and used their data to infer turbulent energy dissipation rate in the stratosphere. Rocket measurements have been able to produce detailed spectra of ion density fluctuations, (Figures 13 and 14) [Royrvik and Smith, 1984; Thrane et al. 1987], neutral species fluctuations, and mass spectrometer measurements [Luebken et al., 1987] Whilst not always showing the classic $k^{-5/3}$ Kolmogroff law, most spectra hovered around the mark, and inferences about turbulent energy dissipation rate were possible. Large variability was found, and values were generally in the range 10^{-4} to 10^{-1} Wkg^{-1} above 80 km. Mesospheric radar measurements have also been made, particularly at Adelaide. This

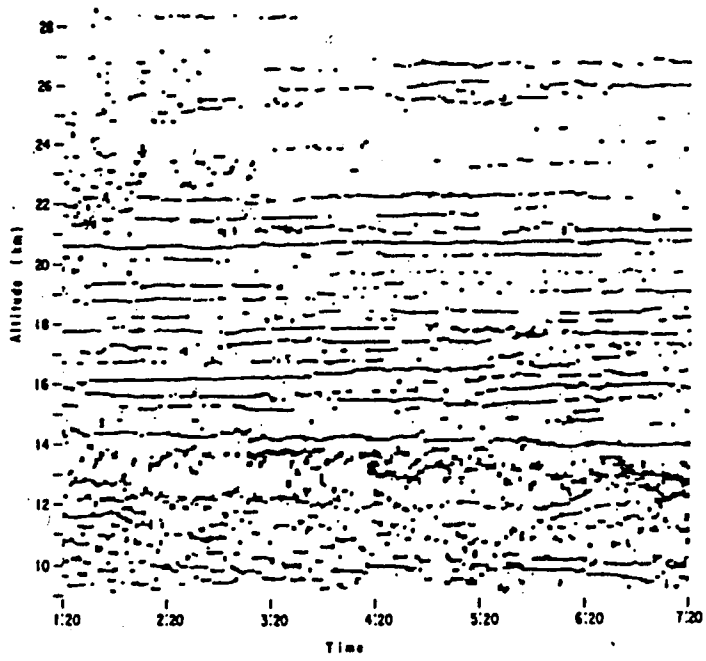

Figure 5. A map showing the evolution of thin turbulent layers over 9 - 28 km from radar observations at Arecibo. [Woodman and Rastogi, 1984].

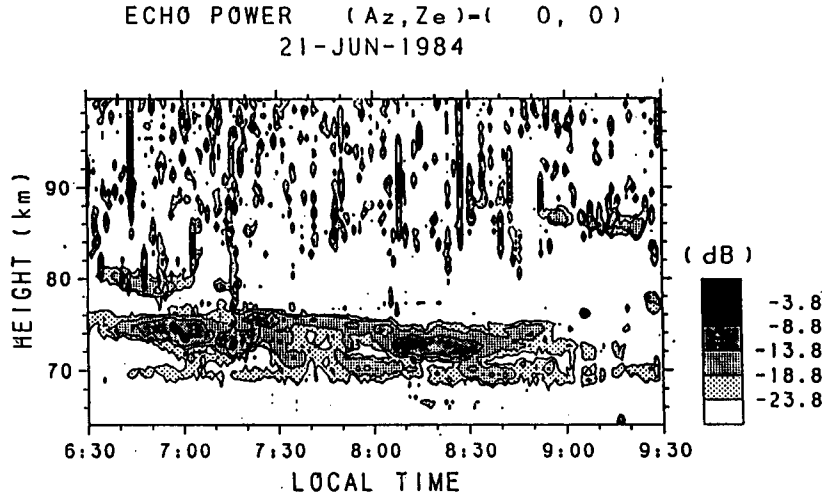

Figure 6. Time-height contour of thermospheric echo power in the vertical beam direction [Sato et al., 1985].

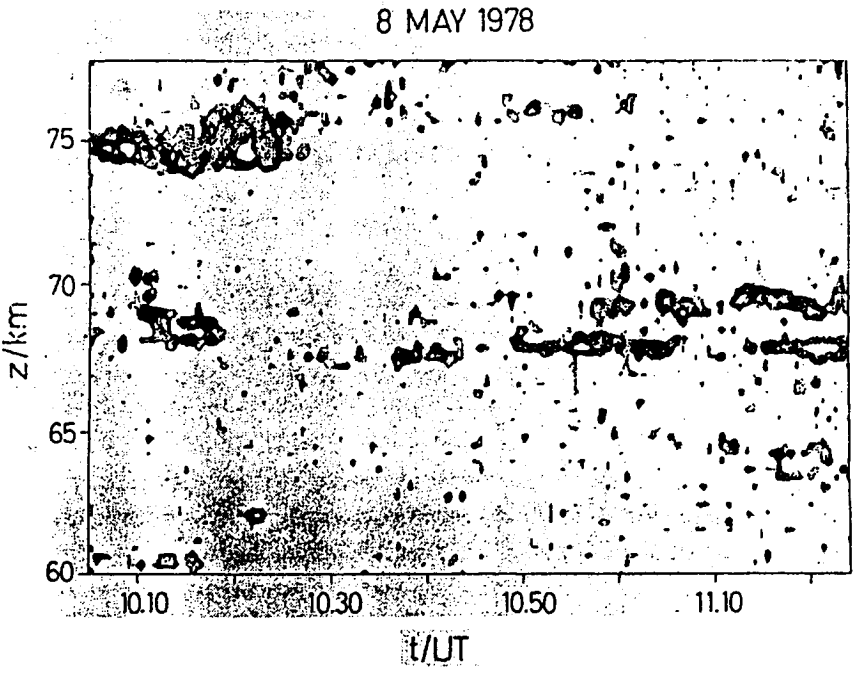

Figure 7.

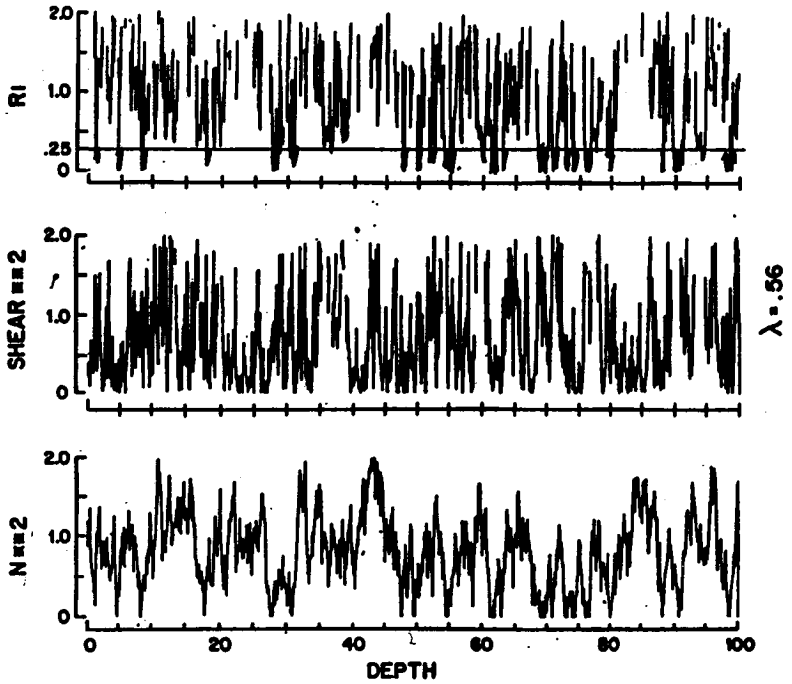

Figure 8. From Desaubies and Smith [1982].

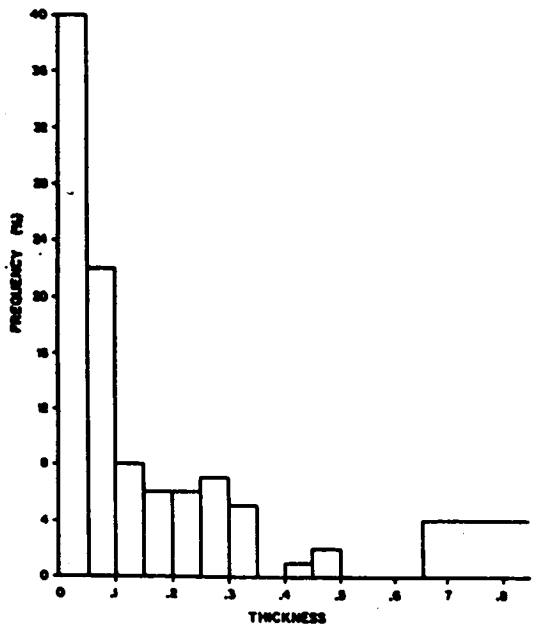

Figure 9. (a) Layer thicknesses. Histogram of the thickness of individual events. Events thicker than 0.65 are in the last bin. Most events are thin and do not contribute to the total energy [Desaubies and Smith, 1982].

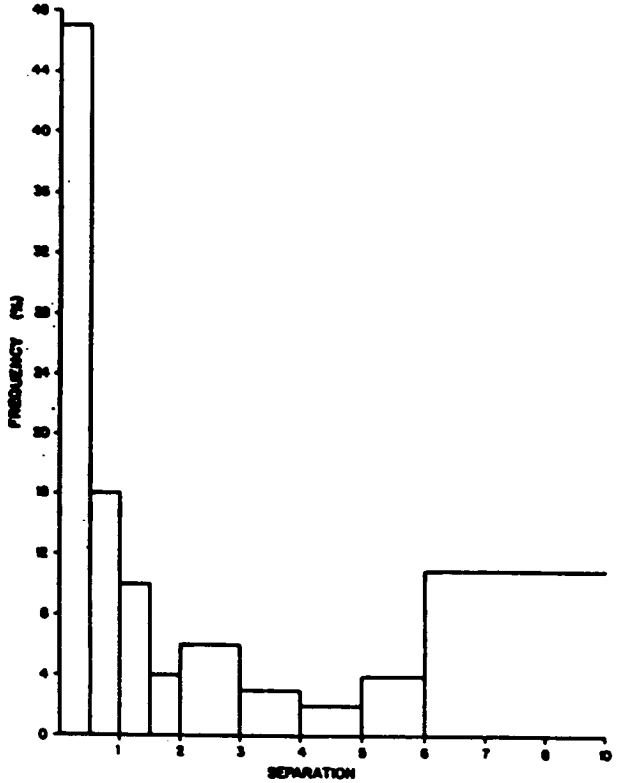

Figure 9. (b) Histogram of separation between events [Desaubies and Smith, 1982].

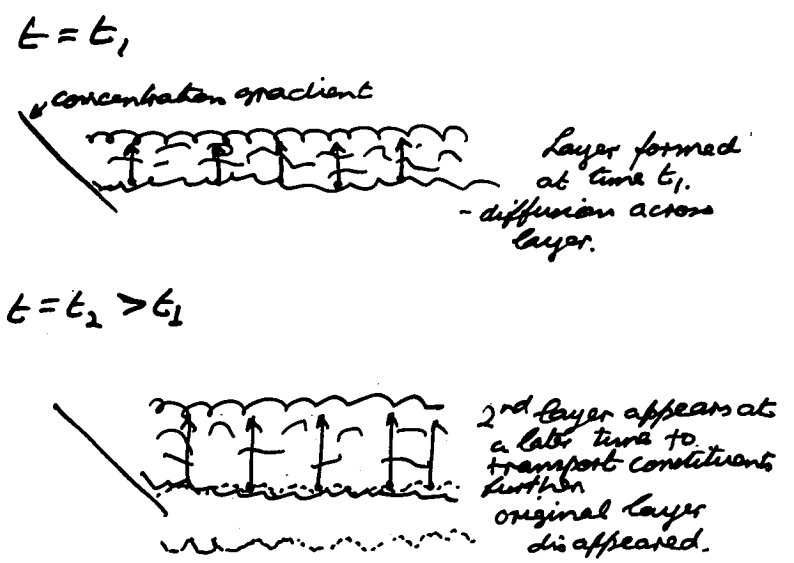

Figure 10.

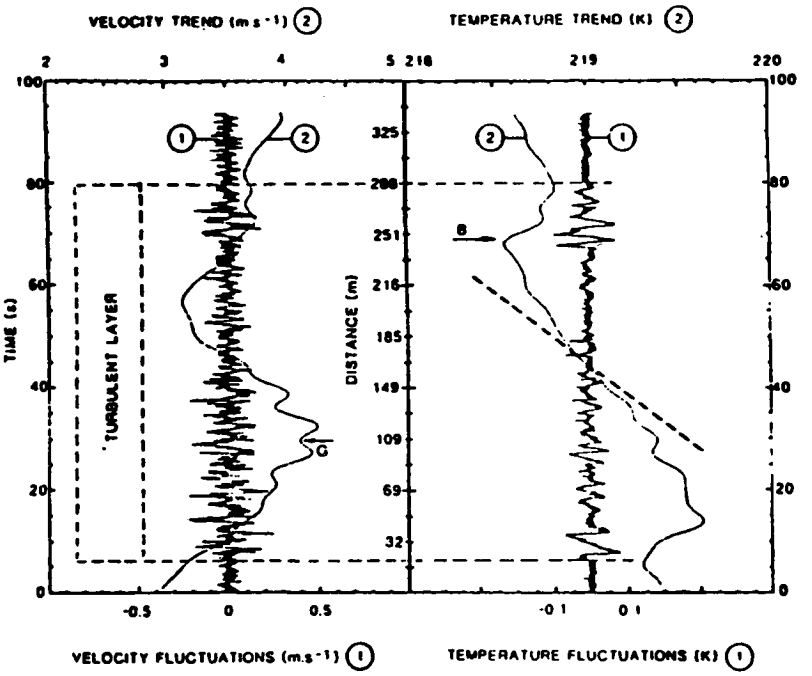

Figure 11. Detailed study of the layer No. 5 both velocity (a) and temperature (b) signals are separated in a fluctuating part (curve 1) and a low frequency part (smooth curve 2). The temperature gradient is near the adiabatic lapse rate (dashed straight line) in the core of the turbulent layer.

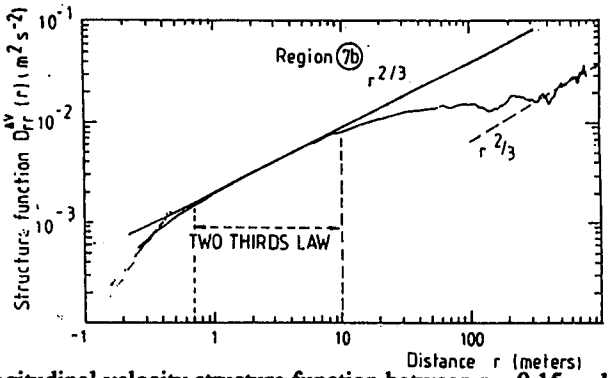

Figure 12. The longitudinal velocity structure function between r = 0.15 and 800 m. A gap occurs around r = 100 m. Measurement is made in a 35 m thick layer while the total turbulent layer 7 is 240 m thick.

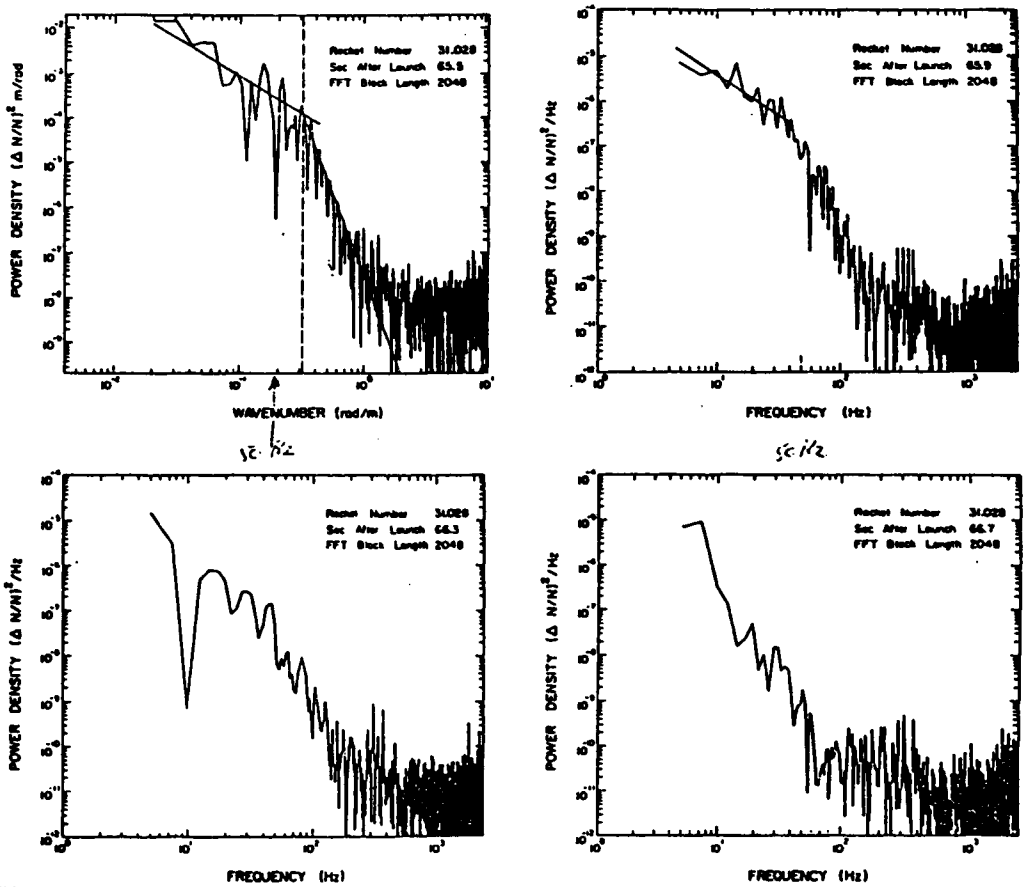

Figure 13. Spectra of relative electron density variations (ΔN/N) in the scattering layer observed by the probe experiment on February 27, 1983 between 85.2 and 86.6 km altitude. The first spectrum has been shown in units of wavelength assuming a rocket velocity of 1.5 km. The three remaining spectra are in units of hertz. The last spectrum is from a region of no detectable turbulence. [Royrvik and Smith, 1984].

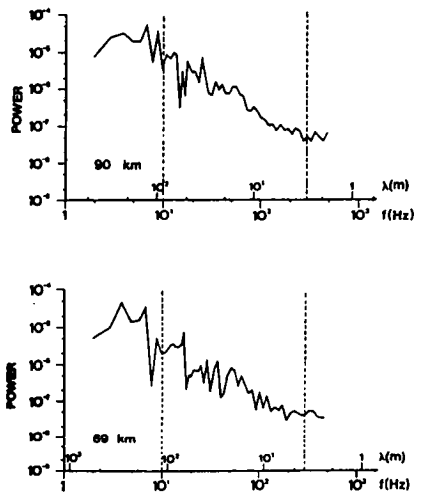

Figure 14. Power spectra P(f) of the ion density fluctuations $\delta N_i/(N_i)$ for four different height intervals centered at 69, 90, 105, and 109 km. The broken lines indicate the estimated limits of useful observations. The upper abcissa scale indicates possible length scales of the fluctuations [Thrane et al., 1985].

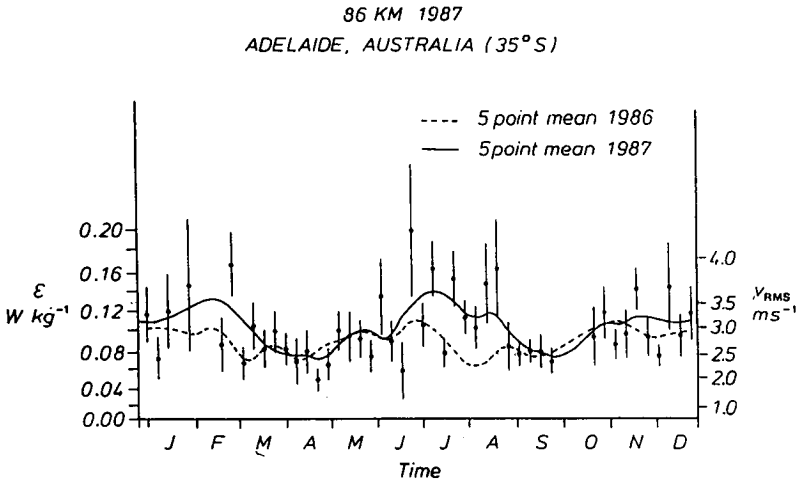

Figure 15.

represents the largest data set at any one site, with data being recorded between 80 and 95 km continuously at 2-h intervals for 3 years (Figure 15).

Figure 16 shows a diagram of the distributions of turbulent energy dissipation rates in the 80 – 120 km altitude region, using data up to about 1983. Subsequent measurements suggest that the shaded region would probably better indicate typical values. A region of very small values around the mesopause has also been noted in a variety of measurements.

The boundary of transition between regions where diffusion is turbulently controlled, and where it is viscously controlled (the turbopause) has also been investigated during MAP, particularly by Russian workers (e.g., Danilov [1984] Figure 17), but its detailed seasonal variation is still poorly understood.

Radar measurements of energy dissipation rates have also been made in the troposphere, by utilizing both absolute backscatter techniques [VanZandt et al., Gage et al., 1980; Weinstock, 1978a,b] (Figure 18), and also using spectral width methods (Figure 19) e.g., Sato and Woodman [1982]; Hocking [1983].

At this view-level, several other advances have been made. Theoretical studies by Weinstock [1981], Dalaudier and Sidi [1987], and Hill and Clifford [1978], etc. have also helped in understanding the energetics and spectral appearance of the turbulent regions. They have helped delineate boundaries between the inertial and buoyancy range of turbulence, for example, and clarified understanding of the energy transfer processes between these ranges.

5. Fine Structure

To really understand turbulence properly, however, requires better knowledge of the fine-scale structure. Although we call it isotropic, individual density structures are far from isotropic. In a stably stratified environment, intense mixing produces a mixture of irregular shapes, and as the driving source of the turbulence becomes less effective, the density inhomogeneities tend to settle out into a horizontally layered structure of interleaved fine scales. Figure 20 shows an example of decaying turbulence in a salt-stratified solution, and Figure 21 shows recent results due to McEwan [1983a,b]. Both show the tendency for the turbulence to stretch out horizontally and "laminate" as the turbulence dies. It seems that the turbulence does not normally force the background state to alter substantially, although some modification takes place. The energetics are such that turbulence must act for some time to be able to drive a layer towards adiabatic.

Theoretical modeling also shows a tendency for the generation of horizontal interleaved structures. For example, a closure model employed by Sykes and Llewellen [1982] has shown the tendency for stratified structures to develop (Figure 22). Simulations of K-H vortices by Klaassen and Peltier [1985a,b] also have shown a tendency for interleaved structures in temperature to develop as a result of the turbulence (Figure 23).

That stratification and turbulence do coexist has been shown by radar measurements. In 1980 Woodman et al. [1981] presented evidence for this at the URSI meetings in Washington, and more recently Hocking [1987] has shown that this can occur using the Adelaide 2 MHz radar (Figure 24).

6. New Perspectives

There are always new ways of visualizing turbulence, and new aspects to its interpretation. One recent advance concerns the process of large-scale diffusion in the atmosphere. We have already seen earlier proposals to explain how large-scale diffusion occurs in the atmosphere, but an important new model has also been developed. A gravity wave carries parcels of air in an elliptical orbit and returns it (almost) to its start position after one cycle. But detailed analysis shows that this is not actually true. In fact the particle drifts

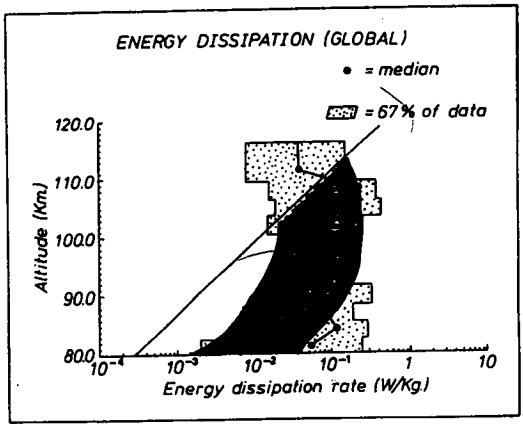

Figure 16. From Hocking [1987].

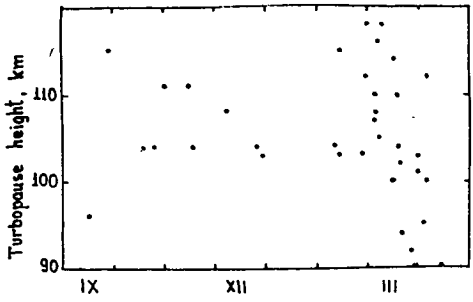

Figure 17. Turbopause height measured at Heiss Island versus season [Danilov, 1984].

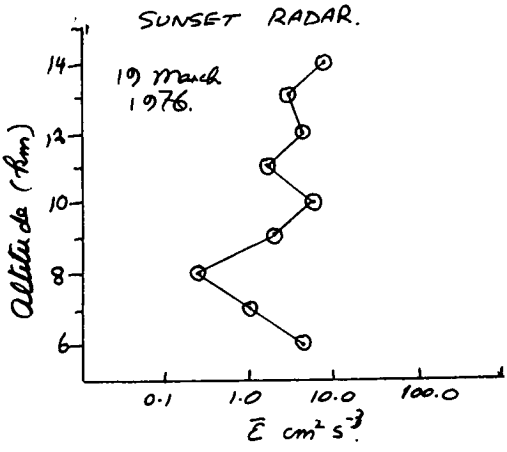

Figure 18. From Gage et al. [1980].

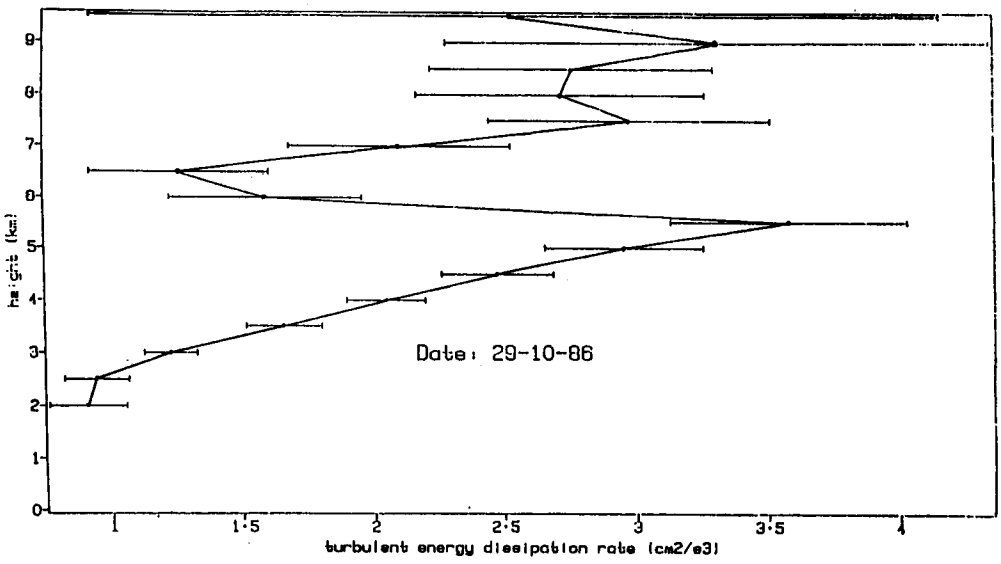

Figure 19. Adelaide.

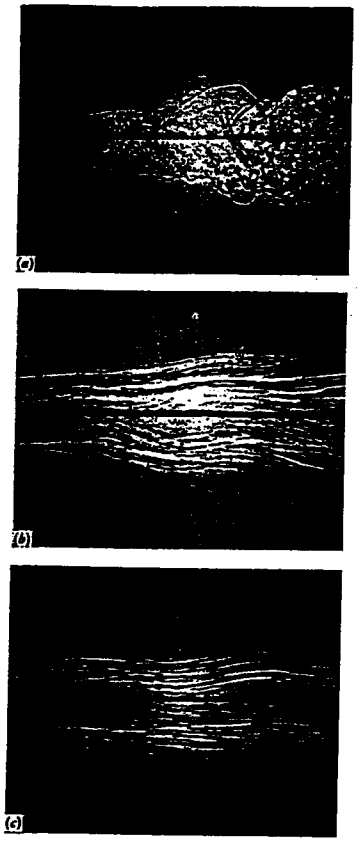

Figure 20. Shadowgraph pictures of a tubulent wake behind a circular cylinder in a stratified fluid (a) near the body: the wake resembles that in a homogeneous fluid. (b) 50 diameters behind the body: the large scale motions have been damped. (c) 100 diameters behind the body: the fine structure has also decayed leaving horizontal striations of concentrations (From Pao [1968] Boeing Scientific Labs., Document DI-82-0959, presented at Symposium on Clear Air Turbulence and its Detection, Seattle, WA, 1968).

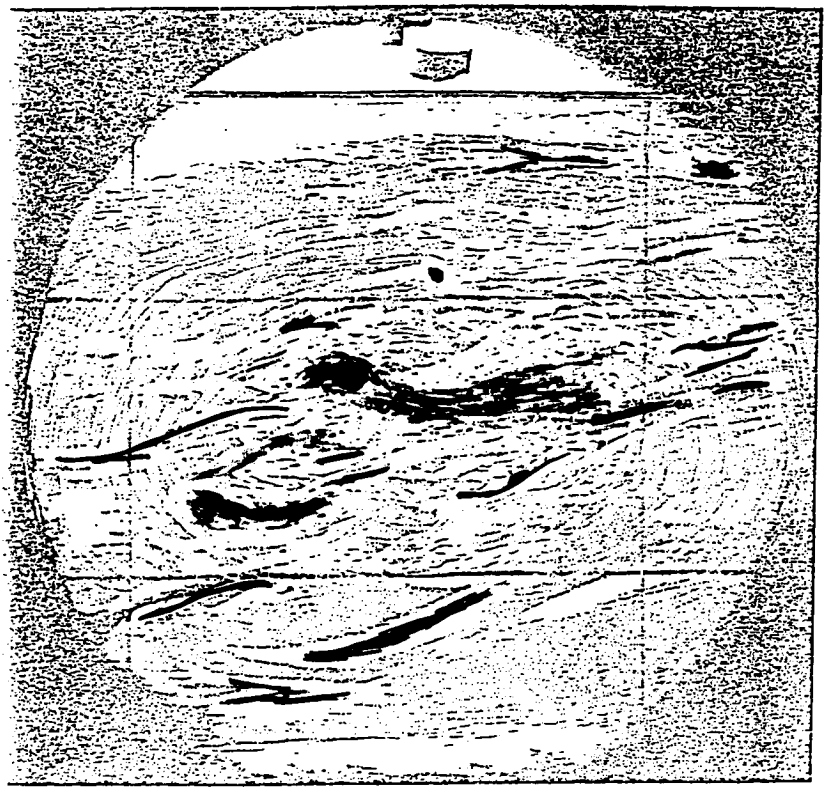

Figure 21. From McEwan [1983].

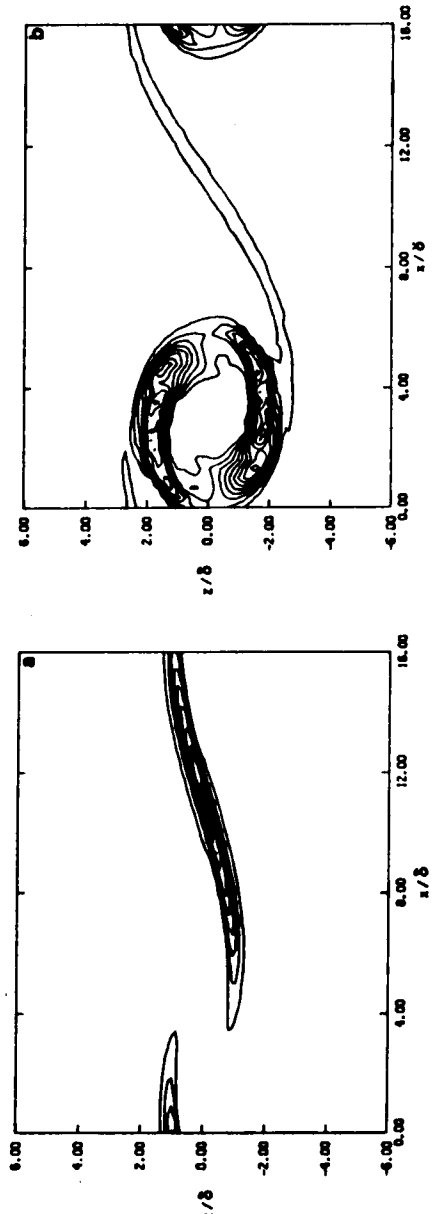

Figure 22. Isopleths of dimensionless temperature variance $\theta^2/\Delta T^2$ for the case with Ri = 0.1; (a) r = 3.0, (b) 4 = 4.9, (c) r = 6.9, (d) r = 9.7. Contour intervals are (a) 0.0005, (b) 0.03, (c) 0.02, (d) 0.004 [Sykes and Lewellen, 1982].

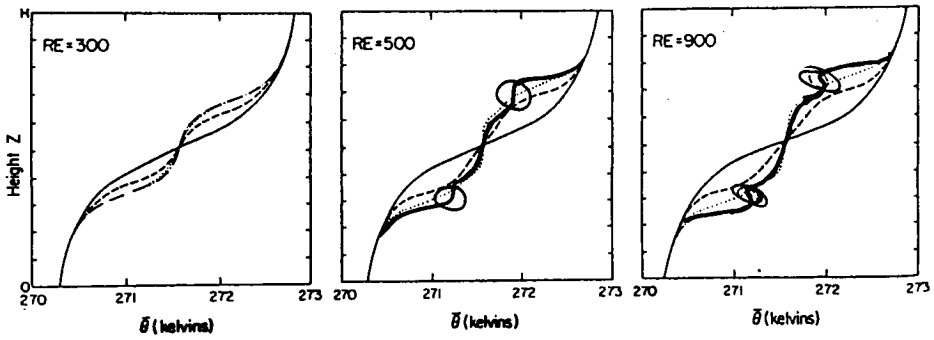

Figure 23. Evolution of the mean velocity defect profile ūz,t) – u′(z) for Re = 300, 500, and 900 KH waves. The profiles are shown at the key times (1) solid, (3) dashed, (5) dot-dashed, and (7) dotted. For Re = 300, key times (5a) and (7b) were used [Klaassen and Peltier, 1985].

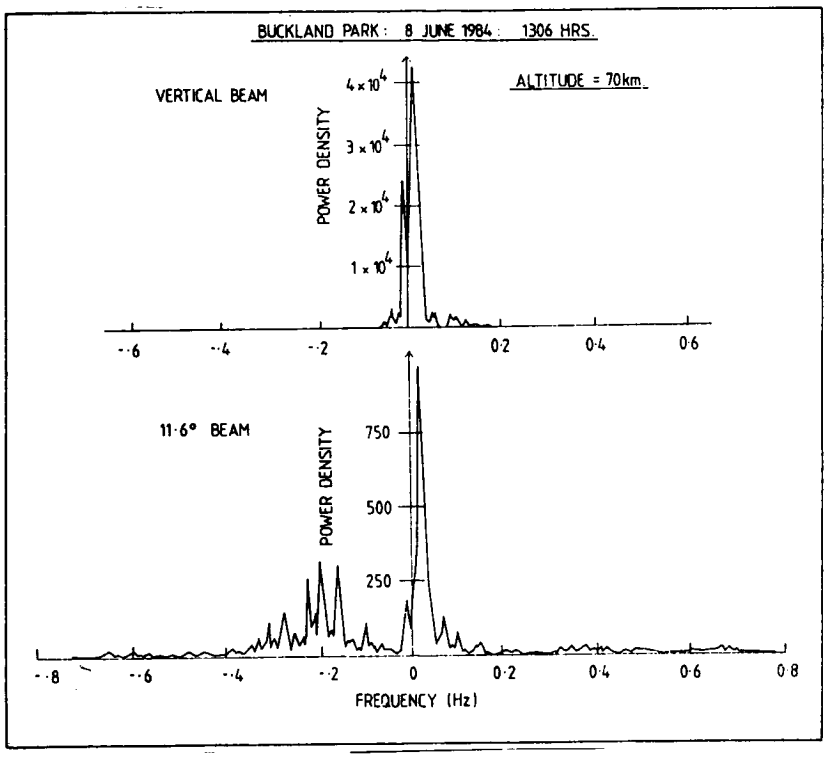

Figure 24. From Hocking [1987].

slightly from its start position, and this constitutes a so-called "Stokes drift". This is true even for nondissipating waves, but more so for dissipating ones.. Figure 25 shows a typical particle "orbit" due to the influence of several waves. When one has a spectrum of waves, the "Stokes drifts" of the waves add in a random-like manner to produce a sort of random walk. The result is a dispersion of an initially compact cloud of particles (Figure 26). This process gives effective diffusion coefficients (for whatever defining such a parameter is worth!) of $\sim 100 - 200\ m^2 s^{-1}$. This process may be a major means of large-scale diffusion in the middle atmosphere. Other recent advances include studies by Kelley et al. [1987, 1988] which have shown that the electron density inertial range extends to scales much smaller than those for neutral fluctuations, at least in the case of high Schmidt number. This is another important area of study to be continued.

REFERENCES

Barat, J., *J. Atmos. Sci., 39*, 2553-2564, 1982.

Colegrove, F. D., W. B. Hanson, and F. S. Johnson, *J. Geophys. Res., 70*, 4931-4941, 1965.

Dalaudier, F., and C. Sidi, *J. Atmos. Sci., 44*, 3121-3126, 1987.

Danilov, A. D., *Adv. Space Res., 4*, 67-78, 1984.

Desaubies, Y., and W. K. Smith, *J. Phys. Oceanography*, 1245, 1982.

Dewan, E.M., *Science, 211*, 1041-1042, 1981.

Fritts, D. C., and T. J. Dunkerton, *J. Atmos. Sci., 42*, 549-556, 1985.

Fritts, D. C., and P. K. Rastogi, *Radio Sci., 16*, 1401-1406, 1985.

Gage, K. S., J. L. Green, and T. E. VanZandt, *Radio Sci., 15*, 407-416, 1980.

Garcia, R. R., and S. Solomon, *J. Geophys. Res., 90*, 3850-3868, 1985.

Groves, G. V., *J. Atmos. Terr. Phys., 48*, 563-571, 1986.

Hill, R. J., and S. F. Clifford, J. *Opt. Soc. Am., 68*, 892-899, 1978.

Hocking, W. K., *J. Atmos. Terr. Phys., 45*, 89-102, 1983a.

Hocking, W. K., J. *Atmos. Terr. Phys., 45*, 103-114, 1983b.

Hocking, W. K., *Adv. Space Res., 7*, 171-181, 1987.

Johnson, F. S., and E. M. Wilkins, *J. Geophys. Res., 70*, 1281-1284, 1965.

Kelley, M. C., D. T. Farley, and J. Rottger, *Geophys. Res., Lett., 14*, 1031-1034, 1987.

Klaassen, G. P., and W. R. Peltier, *J. Fluid Mech., 155*, 1-35, 1985a.

Klaassen, G. P., and W. R. Peltier, *J. Atmos. Sci.*, 1321-1339, 1985b.

Luebken, F. J., U. von Zahn, E. V. Thrane, T. Blix, G. A. Kokin, and S. V. Pachomov, *J. Atmos. Terr. Phys., 49*, 863-869, 1987.

McEwan, A. D., *J. Fluid Mech., 128*, 47-57, 1983a.

McEwan, A. D., *J. Fluid Mech., 128*, 59-80, 1983b.

Royrvik, O., and L. G. Smith, *J. Geophys. Res., 89*, 9014-9022, 1984.

Sato, T., and R. F. Woodman, *J. Atmos. Sci., 39*, 2656-2552, 1982.

Strobel, D. F., M. E. Summers, R. M. Bevilacqua, M. T. Deland, and M. Allen, *J. Geophys. Res., 92*, 6691-6698, 1987.

Sykes, R. I., and W. S. Lewellen, *J. Atmos. Sci., 39*, 1506-1520, 1982.

Thrane, E. V., O. Andreassen, T. Blix, B. Grandal, A. Brekke, C. R. Philbrick, F. J. Schmidlin, H. U. Widdel, U. von Zahn, and F. J. Luebken, *J. Atmos. Terr. Phys., 47*, 243-250-1985.

Weinstock, J., *J. Atmos. Sci., 35*, 1022-1027, 1987a.

Weinstock, J., *J. Atmos. Sci., 35*, 634-49, 1978b.

Weinstock, J. *Radio Sci., 16*, 1401-1406, 1981.

Woodman, R. F., J. Rottger, T. Sato, P.Czechowsky, and G. Schmidt, paper presented at URSI Conf., Washington, August, 1981.

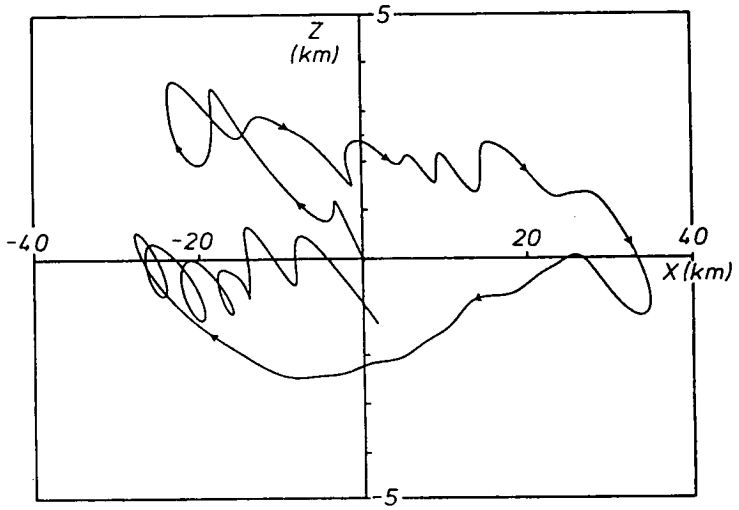

Figure 25.

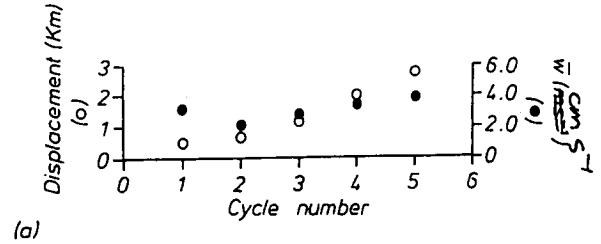

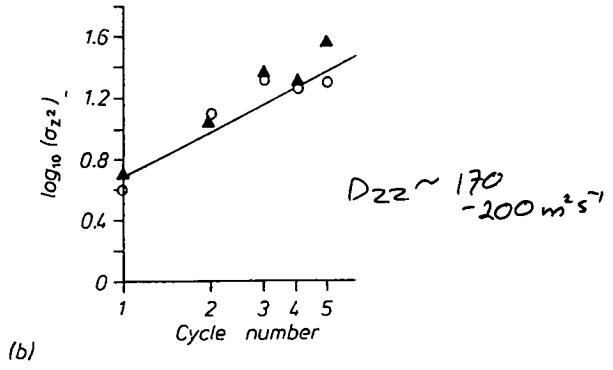

Figure 26.